How Phase Errors Influence Phase-Dependent Amplitudes in Near-Field RISs?

Ke Wang[1,2], Rongbin Chen[1], Chan-Tong Lam[2], Benjamin K. Ng[2], and Chaorong Zhang[2]
[1]*College of Information Engineering, Jiangmen Polytechnic, Jiangmen, China*
[2]*Faculty of Applied Sciences, Macao Polytechnic University, Macao S.A.R, China*
Emails: ke.wang@mpu.edu.mo, chen_rong@ahsgs.uum.edu.my,{ctlam; bng; chaorong.zhang}@mpu.edu.mo

***Abstract*—Near-field reconfigurable intelligent surfaces (RISs) are unlocking promising potentials for the next generation of communications. Different from prior works that separately address phase shifts with errors and phase-dependent amplitudes (PDAs) in the RIS pixel hardware, this paper jointly studies power losses (PLs) caused by these two impairment factors. We propose three different pixel reflection models to accommodate different practical scenarios and derive their approximated upper bounds on the PL. It is important to note that neglecting uncertainties in the PDA may lead to an overestimation of the performance improvement offered by the RIS, thereby explaining the discrepancy between analytical and measurement results in several previous studies. Numerical simulations verify the correctness of the theoretical results.**

***Index Terms*—Reconfigurable intelligent surface, near-field communication, phase-dependent amplitude, power loss, phase error**

I. Introduction

Reconfigurable intelligent surfaces (RISs) hold significant potential to revolutionize wireless communication technologies [1]. Traditional investigations on the RIS have predominantly concentrated on far-field (FF) scenarios [2], which are suitable for long transmission distances. Recently, however, the RIS deployed in near-field (NF) environments has exhibited distinct advantages over alternative transmission enhancement methodologies [3]. The NF RIS not only amplifies the number of reflective pixels but also induces a substantial transformation in electromagnetic characteristics, thereby enhancing spectral efficiency (SE) and spatial degrees of freedom [4].

It should be noted that we cannot consider every pixel of the NF RIS as identical, since each pixel possesses its unique transmission angle and distance [3], [4]. Consequently, the hardware characteristics of each NF RIS pixel must be individually taken into account. Moreover, in practical scenarios, *phase errors (PEs)* within the RIS cannot be overlooked [5]. Previous studies [5]–[7] primarily focused on *phase shift with errors (PSEs)*, represented as[1] $\exp(-\jmath(\phi+\delta))$ where ϕ denotes a controlled phase shift, δ represents the PE following specific distributions, $\exp(\cdot)$ is exponential function, and $\jmath \triangleq \sqrt{-1}$. However, the actual pixel reflection coefficient exhibits its own *phase-dependent amplitudes (PDAs)* [8]–[11], which can be expressed as $\beta(\phi+\delta)$ with $\beta(\cdot) \in (0,1]$ being a nonlinear function. Therefore, the focus of this paper is to explore *How do the PSE and the PDA (with/without the PE) jointly affect the system performance?*

Given the background mentioned above, the motivation for this paper is summarized in Table I. In particular, although many previous works have explored the impacts of the PSE and/or the PDA (without the PE) on the RIS-aided system [4]–[13], there is no research on the mutual coupling of these two attenuation factors, especially when the PDA contains the PE. It should be emphasized that the pixel hardware is increasingly vulnerable as it incorporates sophisticated tuning, control, and sensing systems [14]. For example, varactor diodes in Fig. 1 may produce high current densities, potentially causing electromigration within the device [15]. Thus, from a practical perspective, the PDA may also exist the PE. It is noteworthy that this omission may be pivotal in accounting for the disparity between theoretical analyses and hardware validations [16]. Therefore, different from the existing FF pixel reflection models (i.e., Perfect, Cases I and II in Table I), a more practical NF model (i.e., Case III in Table I) is imperative for future performance analyses and algorithm designs for the RIS-assisted system.

Model	Works	PSE	PDA
Perfect	[4], [12], [13]	$\exp(-\jmath\phi)$	1
Case I	[5]–[7]	$\exp(-\jmath(\phi+\delta))$	$\beta \in (0,1]$
Case II	[8]–[11]	$\exp(-\jmath(\phi+\delta))$	$\beta(\phi) \in (0,1]$
Case III	This paper	$\exp(-\jmath(\phi+\delta))$	$\beta(\phi+\delta) \in (0,1]$

TABLE I: Related works with different pixel reflection models.

In this paper, our contributions are as follows:

- We initially showcase the hardware configuration of the RIS pixel, followed by an investigation of the impact of different parameters on the approximated PDA model. Then, we derive the lower and upper bounds of the ideal PDA without any PEs.
- Second, we introduce a useful metric named *power loss (PL)* to assess the energy conservation of each RIS pixel. Then, three different pixel reflection models are proposed to accommodate distinct practical scenarios, and new approximated polynomial form upper bounds on the PL are also derived.
- Third, based on the Friis transmission formula and the proposed complete/incomplete reflection models, a new light-of-sight (LoS) NF channel model, is derived. We confirm its effectiveness through numerical assessments.

[1]If ϕ is optimally continuous, $\exp(-\jmath(\phi+\delta))$ is equivalent to $\exp(-\jmath\delta)$ since the phase of the cascade path and ϕ cancel each other out. [2].

The rest of the paper is organized as follows. Sec. II introduces the pixel hardware structure and its approximated PDA. Then, in Sec. III, three different pixel reflection models and their upper bounds on the PL are proposed. Channel model and simulation results are provided in Sec. IV. We finally conclude this work in Sec. V.

Notation: $|\cdot|$ denotes absolute value, $\|\cdot\|$ is l_2 norm, $[\cdot]^{\mathsf{T}}$ is transpose operation. Besides, $\sin(\cdot)$ and $\cos(\cdot)$ are respectively sine and cosine functions. Moreover, $\mathcal{CN}$, $\mathcal{UF}$, and $\mathsf{E}\{\cdot\}$ represent complex Gaussian distribution, uniform distribution, expectation function, respectively.

II. Phase-Depended Amplitudes in RIS Pixels

In this section, we start by elucidating the hardware configuration of the RIS pixel. Henceforth, an examination of the approximated PDA is studied.

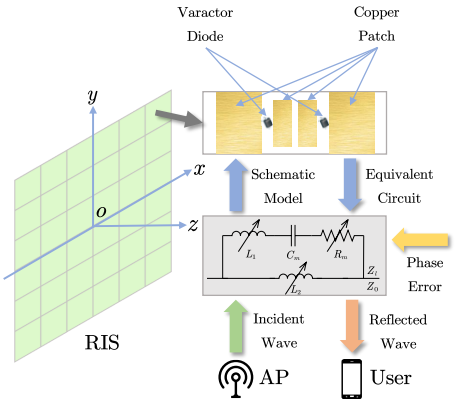

Fig. 1: Top view schematic of the RIS pixel and its simplified equivalent circuit model.

A typical RIS pixel hardware contains three layers [16]. As shown in Fig. 1, the top layer contains two pairs of copper patches, each of which is connected by a varactor diode. The middle layer is a complete metallic panel, for reflecting incoming waves and preventing energy loss, and the bottom layer consists of direct current biasing lines. A single pixel can be modeled as a parallel resonant circuit.

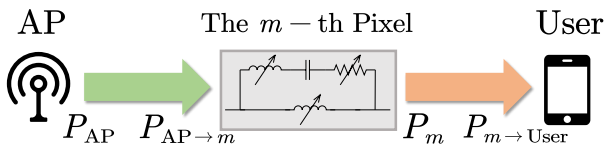

Fig. 2: A downlink cascaded path of the m-th pixel.

Fig. 2 illustrates a downlink cascaded path of the RIS-aided communication. If the RIS as M pixels, and $m = 1, \ldots, M$, then P_{AP}, $P_{\mathrm{AP}\to m}$, P_m, and $P_{m\to \mathrm{User}}$ denote the transmit power by the AP, the received power by the m-th pixel, the reflected power by the m-th pixel, and the received power by the user. Note that $P_{\mathrm{AP}\to m} \geq P_m$ since there always exists energy loss when the pixel reflects the wave [1]. In particular, for the m-th pixel, an ideal equivalent low-pass receiver power can be obtained as

$$P_m = \left|\beta(\phi_m)\exp(-\jmath\phi_m)\right|^2 P_{\mathrm{AP}\to m}, \tag{1}$$

where $\beta(\phi_m)$ is the m-th PDA of the pixel and ϕ_m is the desired pixel phase shift.

Most previous works ignored the amplitude $\beta(\phi_m)$ or simply assumed it is a constant smaller or equal one [4]–[7], [12], [13]. This makes sense if we consider the FF scenario and each pixel works in the same behavior. However, if the transceiver and the RIS in the near field, the pixel has its own feature. In other words, given the different transmission distances between the pixels and the transceiver, we have to not only consider the different phases but also the different distances and other unique characteristics such as the PDA of each scatterer. Let ς_m represent the equivalent circuit, then [8] introduced an amplitude model as

$$\beta(\phi_m) = (1-b)\cdot\left(\frac{\sin(\phi_m - c)+1}{2}\right)^a + b, \tag{2}$$

where $a \geq 1$ is the steepness factor, $b \in [0,1]$ is the minimum amplitude, $c > 0$ is the horizontal distance between $\pi/2$ to π, and all parameters are related to the specific circuit implementation. We call $\beta(\phi_m)$ in (2) as *approximated phase-depended amplitude*.

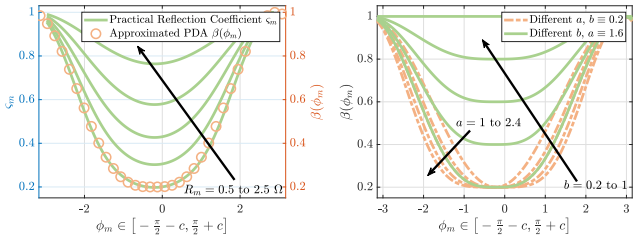

(a) Approximated PDA model. (b) Different b and a.

Fig. 3: Approximated PDA model validations and the impacts by different parameters a and b. Other electrical parameters can be found in [8].

Fig. 3a shows the relationship between phase shift $\phi_m \in \left[-\frac{\pi}{2}-c, \frac{\pi}{2}+c\right]$ and reflected amplitude $\beta(\phi_m) \in [b, 1]$. When ϕ_m approaches $\pm(\frac{\pi}{2}+c)$, the amplitude $\beta(\phi_m)$ is maximized. This is because the reflective currents are out-of-phase with the element currents. Accordingly, when $\phi_m = -\frac{\pi}{2} + c$[2], the amplitude is minimized to b since the dielectric and metallic losses increase. From Fig. 3b, it can be observed that the minimum amplitude b is more important than the other parameters[3], i.e., a and c. We then have a proposition as follows.

[2]It's worth mentioning that there is no negative phase in reality, thus for ϕ_m, the actual phase shift should add $2k\pi$ where k is a non-negative integer. However, we omit $2k\pi$ in this paper.

[3]For example, when b is fixed to 0.5, the PL between $a = 1.6$ and 2 is just 0.2 dB. However, if a equals 2, the PL between $b = 1$ and 0.5 is 3.2 dB. More details can be found in [8].

Proposition 1 (Lower and upper bounds of the ideal PDA): *When the pixel hardware and the phase shift are ideal, then the lower and upper bounds of $\beta(\phi_m)$ in (2) can be obtained as*

$$b \overset{(i)}{\leq} \beta(\phi_m)\big|_{a>1} \overset{(ii)}{\leq} \beta(\phi_m)\big|_{a=1} \overset{(iii)}{\leq} 1. \tag{3}$$

Proof: First, when $\phi_m = -\frac{\pi}{2} + c$, (i) holds equality. Similarly, (ii) is the equal sign when $\beta(\phi_m)$ is minimized (maximized). Besides, since $\sin(\phi_m - c) \in [0,1]$ and $b \in [0,1]$, it is not difficult to verify that (iii) is correct, hence we finish the proof. ∎

Remark 1: *Previous works assumed full pixel reflections, which cannot be obtained in reality. Instead of focusing on $\beta(\phi_m)\big|_{a>1}$, b and 1, we mainly study $\beta(\phi_m)\big|_{a=1}$ in the rest of this paper, and this can be regarded as a special case of the proposed model $\beta(\phi_m)$. Consequently, we assume in the remaining part of this paper that $\bar{\beta}(\phi_m) = \beta(\phi_m)\big|_{a=1}$. Given that a is less significant relative to other parameters, $\bar{\beta}(\phi_m)$ is indicative of the predominant characteristic of $\beta(\phi_m)$.*

III. Impacts by Introducing Phase Errors into Phase-Dependent Amplitudes

In Sec. II, we introduce the RIS pixel hardware structure and its approximated equivalent model. In practice, however, the PE can not be ignored since it not only present in the PSE but also a significant factor in the PDA. The PE is caused by multiple internal and/or external reasons such as hardware degradations, channel estimations, and human-induced accidents [5]–[7], [11]. Hence, in this section, we delve into the last three scenarios outlined in Table I, with a particular focus on the implications of integrating the PE with the PDA, i.e., Case III.

A. Phase Errors in RIS Pixels

We assume that the PE δ_m in the m-th pixel follows a uniform distribution[4], i.e., $\delta_m \sim \mathcal{UF}[-x, x]$, where $x \in [0, \pi/2]$, and the probability density function is $f(\delta_m) = \frac{1}{2x}$ when $\delta_m \in [-x, x]$ or is zero otherwise. Then the practical pixel reflection coefficient is[5] $\beta(\phi_m + \delta_m)\exp(-\jmath(\phi_m + \delta_m))$.

Suppose there is an RIS with M pixels and each transceiver equips a single isotropic antenna. The whole power that is emitted from the RIS can be obtained as $P_{\text{RIS}} = \left|\sum_{m=1}^{M} \sqrt{P_{\text{AP}\to m}}\beta(\phi_m + \delta_m)\exp(-\jmath(\phi_m + \delta_m))\right|^2$. Consider we have perfect channel state information, then the PSE $\exp(-\jmath(\phi_m + \delta_m))$ is equivalent to $\exp(-\jmath\delta_m)$. Hence P_{RIS} can be rewritten as

$$\begin{aligned} P_{\text{RIS}} &= \left|\sum_{m=1}^{M} \sqrt{P_{\text{AP}\to m}} \overbrace{\beta(\phi_m + \underbrace{\delta_m}_{\text{PE}})}^{\text{PDA}} \overbrace{\exp(-\jmath\underbrace{\delta_m}_{\text{PE}})}^{\text{PSE}}\right|^2 \\ &\overset{(i)}{\approx} P_{\text{AP}\to m}\left|\sum_{m=1}^{M} \beta(\phi_m + \delta_m)\exp(-\jmath\delta_m)\right|^2 \\ &\overset{(ii)}{\approx} \underbrace{M^2 P_{\text{AP}\to m}}_{\text{Square Law}} \underbrace{\left|\mathsf{E}\{\beta(\phi_m + \delta_m)\exp(-\jmath\delta_m)\}\right|^2}_{\text{Power Loss } \Gamma \in (0,1)}, \end{aligned} \tag{4}$$

where (i) and (ii) are respectively obtained when the pixels receive the same transmit power and $M \gg 1$.

Remark 2: *It can be seen that (4) contains two parts. The first one, i.e., $M^2 P_{\text{AP}\to m}$, reveals that the total power emitted from the RIS P_{RIS} increases directly proportional to M^2. This behavior is also called square law in the RIS communication [13]. Moreover, the second part cannot be ignored especially when we consider a practical RIS system. Previous works only considered the PSE loss, i.e., $|\mathsf{E}\{\exp(-\jmath\delta_m)\}|^2$. In the rest of this paper, we consider $\Gamma = |\mathsf{E}\{\beta(\phi_m + \delta_m)\exp(-\jmath\delta_m)\}|^2$ as a more practical one. Besides, it is important to note that $\phi_1 \neq \phi_2 \neq \cdots \neq \phi_M$ given that each pixel experiences its own cascaded fading channel in practice, thus it is difficult to obtain a satisfied approximation of Γ in (4). However, we can let $\phi_1 = \phi_2 = \cdots = \phi_M = \phi_m$ when we want to study the general impact of a specific δ_m on P_{RIS}.*

B. Case I: When the Amplitude is a Constant

When the PDA of the m-th pixel is a constant, we then have the PL approximation as follows.

Proposition 2 ($\beta_m\exp(-\jmath\delta_m)$, the PDA is a constant): *When the m-th PDA is a constant β, and the PSE includes $\delta_m \sim \mathcal{UF}[-x, x]$ where $x \in [0, \frac{\pi}{2}]$, then the PL Γ can be obtained as*

$$\begin{aligned} \Gamma_1 &= \left|\mathsf{E}\{\beta_m\exp(-\jmath\delta_m)\}\right|^2 \\ &\overset{(i)}{\approx} \beta^2\left(1 - \frac{1}{3}x^2 + \frac{2}{45}x^4 - \frac{1}{360}x^6 + \frac{1}{14400}x^8\right), \end{aligned} \tag{5}$$

where (i) is attained when $\beta_1 = \beta_2 = \cdots = \beta_m = \beta$ and (5) diminishes when x increases.

Proof: Please see Appendix A. ∎

Remark 3: *Fig. 4a reveals that approximating Γ in Case I needs at least the first three terms of the Taylor series expansion of $\sin(x)$ in Appendix A. The imperfect analytical (AN) case in the figure uses $\sin(x) \approx x - \frac{1}{6}x^3 + o(x^5)$. However, it is not accurate as x approaches $\frac{\pi}{2}$, which leads to a mismatch between AN and Monte Carlo (MC) results.*

C. Case II: When the Amplitude is without Phase Errors

When the PDA of the m-th pixel is not a constant and without δ_m, we have the upper bound of the PL as follows.

Proposition 3 ($\beta(\phi_m)\exp(-\jmath\delta_m)$, the PDA is PE-free): *When the m-th PDA is $\beta(\phi_m)$ and without any PEs, and the*

[4]Normally there are two types of PE in the RIS pixel [5], i.e., imperfect phase estimations and quantization errors, which respectively follow von Mises and uniform distributions. This paper considers the latter since we study from a hardware perspective.

[5]This paper assumes the PSE and the PDA share the same PE δ_m. However, based on Fig. 6d, if these two components have independently and identically distributed (i.i.d.) δ_m, the performance degradation will be more pronounced. This is left open for future investigations.

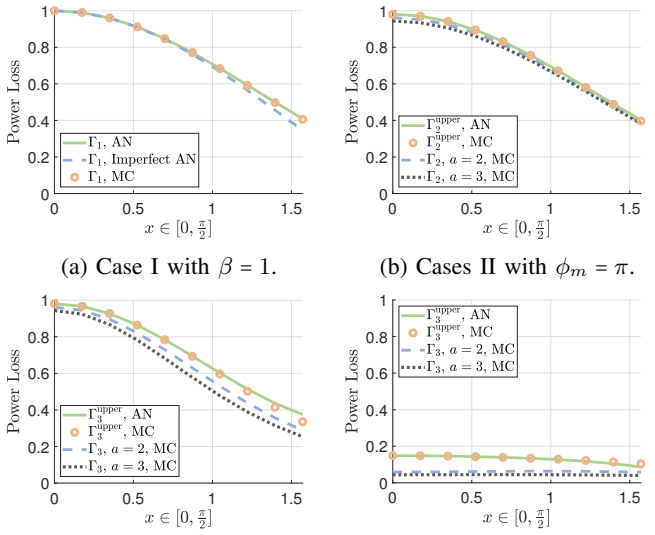

(a) Case I with $\beta = 1$. (b) Cases II with $\phi_m = \pi$.

(c) Cases III with $\phi_m = \pi$. (d) Cases III with $\phi_m = \frac{\pi}{4}$.

Fig. 4: The PL Γ in Cases I, II, and III with $\phi_m = \pi$ or $\frac{\pi}{2}$, $b = 0.2$, and $c = 0.43\pi$. The realization number is 5000.

PSE includes $\delta_m \sim \mathcal{UF}[-x, x]$ *where* $x \in \left[0, \frac{\pi}{2}\right]$, *then the upper bounds of the PL can be obtained as*

$$\Gamma_2 \le \Gamma_2^{\text{upper}} \approx \zeta\left(1 - \frac{1}{3}x^2 + \frac{2}{45}x^4 - \frac{1}{360}x^6 + \frac{1}{14400}x^8\right), \quad (6)$$

where $\Gamma_2 = \left|\mathsf{E}\{\beta(\phi_m)\exp(-\jmath\delta_m)\}\right|^2$, $\Gamma_2^{\text{upper}} = \left|\mathsf{E}\{\bar{\beta}(\phi_m)\exp(-\jmath\delta_m)\}\right|^2$, $\zeta = \frac{(1-b)^2}{4}\sin^2(\phi_m - c) + \frac{(1-b^2)}{2}\sin(\phi_m - c) + \frac{(1+b)^2}{4}$, *and* (6) *decreases when* x *increases.*

Proof: Please see Appendix B. ∎

Remark 4: *It is not difficult to find that* $b^2 \le \zeta \le 1$, *and* b^2 *and* 1 *can be obtained respectively when* $\phi_m = -\frac{\pi}{2} + c$ *and* $\pm\left(c + \frac{\pi}{2}\right)$. *Hence, the minimum upper bound of the PL only depends on* b. *Besides, Fig. 4b reveals that when* x *approaches* 0, $a = 1$ *outperforms others, but they are almost the same when* x *approaches* $\frac{\pi}{2}$. *In other words,* a *in* (2) *is not that important especially when the PE* δ_m *becomes more serious.*

D. Case III: When the Amplitude is with Phase Errors

When the PDA of the m-th pixel is not a constant and with δ_m, we have the upper bound of the PL as follows.

Proposition 4 $\left(\beta(\phi_m + \delta_m)\exp(-\jmath\delta_m)\right.$, the PDA is with the PE$\left.\right)$: *When the* m*-th PDA is* $\beta(\phi_m + \delta_m)$, *and the PDA and the PSE all contain* $\delta_m \sim \mathcal{UF}[-x, x]$ *where* $x \in \left[0, \frac{\pi}{2}\right]$, *then the upper bound of the PL can be obtained as*

$$\Gamma_3 \le \Gamma_3^{\text{upper}} \approx (\eta_1 + \eta_2)^2 + \eta_3, \quad (7)$$

where $\Gamma_3 = \left|\mathsf{E}\{\beta(\phi_m + \delta_m)\exp(-\jmath\delta_m)\}\right|^2$, $\Gamma_3^{\text{upper}} = \left|\mathsf{E}\{\bar{\beta}(\phi_m + \delta_m)\exp(-\jmath\delta_m)\}\right|^2$, $\eta_1 = \frac{(1-b)}{2}\sin(\phi_m - c)\left(1 - \frac{1}{3}x^2 + \frac{1}{15}x^4\right)$, $\eta_2 = \frac{(1+b)}{2}\left(1 - \frac{1}{6}x^2 + \frac{1}{120}x^4\right)$, *and* $\eta_3 = \frac{(1-b)^2}{4}\left(\frac{1}{3}x^2 - \frac{1}{15}x^4\right)^2\cos^2(\phi_m - c)$, *and* (7) *decreases with increasing* x.

Proof: Please see Appendix C. ∎

Remark 5: *From Fig. 4c, it can be seen that the PL differences between* $a = 1, 2$ *and* 3 *are obvious. This is because Case III is not only influenced by the PE* $\exp(-\jmath\delta_m)$ *but also, more importantly, by the PDA* $\beta(\phi_m + \delta_m)$. *Besides, when the amplitude is large (e.g.,* $\phi_m = \frac{\pi}{2} + c$*), the impact of the PE* δ_m *on the PDA is more significant. Fig. 4d shows Case III with* $\phi_m = \frac{\pi}{4}$, *and it can be seen that the PL of* $a = 1, 2$ *and* 3 *are all small and they are not influenced by* δ_m *very seriously. Besides, the mismatches between the AN and MC results in Fig. 4c and 4d are caused by using the Taylor expansion at* $x = 0$ *in Appendix. C.*

IV. Channel Model and Numerical Evaluations

In this section, we first give a LoS channel model of the NF RIS-aided communication considering the PDA with the PE. Then we offer numerical evaluations to show the correctness of our results.

A. Channel Model

Consider a single-input single-output RIS-aided system that includes an access point (AP), a user, and an RIS. The direct link is blocked, the RIS is a planar surface on a rectangular grid spaced d_x and d_y apart in the xoy-plane of a three-dimensional Cartesian coordinate system where o denotes the origin point, and the sizes and the geometric center of the RIS are $\sqrt{M} \times \sqrt{M}$ and $[0, r, 0]^{\mathsf{T}}$, respectively. Besides, we set $d_x = d_y = \lambda/2$ to avoid spatial correlations [4], where λ is wavelength. The position of the AP and user are $D_{\text{AP}} = [x_{\text{AP}}, y_{\text{AP}}, z_{\text{AP}}]^{\mathsf{T}}$ and $D_{\text{User}} = [x_{\text{User}}, y_{\text{User}}, z_{\text{User}}]^{\mathsf{T}}$, respectively. Then the distances between the AP and the m-th element and between the m-th element and the user can be respectively obtained as $d_{\text{AP}\to m} = \|D_m - D_{\text{AP}}\|$ and $d_{m\to\text{User}} = \|D_{\text{user}} - D_m\|$ where D_m is defined in [11]. Accordingly, the time delays are $\tau_{\text{AP}\to m} = d_{\text{AP}\to m}/\nu$ and $\tau_{\text{m}}^{\text{user}} = d_{\text{m}}^{\text{user}}/\nu$, respectively, where ν denotes the speed of light. Using *Friis transmission formula* [17], for the AP-to-pixel path, we have

$$\frac{P_{\text{AP}\to m}}{P_{\text{AP}}} = \left(\frac{\lambda}{4\pi d_{\text{AP}\to m}}\right)^2 G_{\text{AP}} G_{\text{AP}\to m}, \quad (8)$$

where $P_{\text{AP}\to m}$ is the received power of the m-th RIS pixel, which is part of the power that is emitted from the AP, i.e., P_{AP}. Besides, G_{AP} and $G_{\text{AP}\to m}$ are the AP antenna gain and the m-th pixel gain from the direction of the AP. Similarly, for the pixel-to-user path, we have

$$\frac{P_{m\to\text{User}}}{P_m} = \left(\frac{\lambda}{4\pi d_{m\to\text{User}}}\right)^2 G_{\text{User}} G_{m\to\text{User}}, \quad (9)$$

where $P_{m\to\text{User}}$ is the received power of the user, which is part of the power that is emitted from the m-th RIS element, i.e., P_m. It is worth noting that based on (1), the pixel is with the PE and the PDA. Hence $P_{\text{AP}\to m} \ge P_m$. Besides,

G_{User} and $G_{m\to\text{User}}$ are the user antenna gain and the m-th pixel gain from the direction of the user, and [6] $G_{\text{AP}\to m} = \frac{4\pi}{\lambda^2} d_x d_y \cos(\theta_{\text{AP}\to m})$ and $G_{m\to\text{User}} = \frac{4\pi}{\lambda^2} d_x d_y \cos(\theta_{m\to\text{User}})$ where $\theta_{\text{AP}\to m} \in \left(0, \frac{\pi}{2}\right)$ and $\theta_{m\to\text{User}} \in \left(0, \frac{\pi}{2}\right)$, and $G_{\text{AP}} = G_{\text{User}} = 1$. Thus the received signal y can be obtained as

$$y = h \cdot \sqrt{P_{\text{AP}}} \cdot s + \omega, \tag{10}$$

where $h = \sum_m g_m \beta(\phi_m + \delta_m) \exp(-\jmath(\phi_m + \delta_m)) h_m$, the m-th LoS channel of the AP-to-pixel and the pixel-to-user paths are respectively $g_m = A_{\text{AP}\to m} \exp(-\jmath 2\pi f_c \tau_{\text{AP}\to m})$ and $h_m = A_{m\to\text{User}} \exp(-\jmath 2\pi f_c \tau_{m\to\text{User}})$, f_c is carrier frequency, $A_{\text{AP}\to m} = \frac{\lambda}{4\pi d_{\text{AP}\to m}} \sqrt{\pi \cos(\theta_{\text{AP}\to m})}$, and $A_{m\to\text{User}} = \frac{\lambda}{4\pi d_{m\to\text{User}}} \sqrt{\pi \cos(\theta_{m\to\text{User}})}$. Besides, s is an unit-power signal symbol, and $\omega \sim \mathcal{CN}(0, \sigma^2)$ denotes additive white Gaussian noise with the variance σ^2, then the SE can be obtained as

$$\text{SE} = \text{E}\left\{ \log_2 \left(1 + \frac{P_{\text{AP}} \cdot |h|^2}{\sigma^2} \right) \right\}. \tag{11}$$

B. Numerical Evaluations

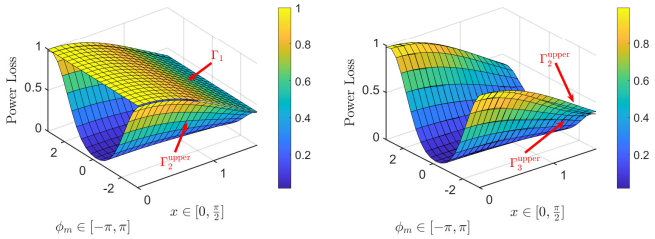

(a) Γ_1 vs. Γ_2^{upper}. (b) Γ_2^{upper} vs. Γ_3^{upper}.

Fig. 5: 3D illustrations comparing different PLs. Note that $b = 0.2$ and $c = 0.43\pi$.

First, we presents 3D illustrations comparing different PLs in Fig. 5. In particular, from Fig. 5a, it can be observed that Γ_1 and Γ_2^{upper} have different 3D patterns. This is because Γ_1 contains the fixed amplitude, rather than the PDA, which is included in Γ_2^{upper}. Fig. 5b shows that the error in the PDA brings an extra performance degradation, and this decrease becomes more serious when ϕ_m approaches $\pm\left(\frac{\pi}{2} + c\right)$. However, when $\phi_m = -\frac{\pi}{2} + c$, all PLs can be ignored.

Secondly, we show how much the PDA (with/without the PE) decrease SE in a realistic setting. Assume the RIS is on the xoy-plane shown in Fig. 1, and it moves slowly from a location near the AP to close the user. The simulation setup parameters are $D_{\text{AP}} = [-8, 15, 8]^{\mathsf{T}}$ m, $D_{\text{User}} = [8, 1.5, 8]^{\mathsf{T}}$ m, the center of RIS is $[x_{\text{RIS}}, 10, 0]^{\mathsf{T}}$ m where $x_{\text{RIS}} \in [-8, 8]$ m. Besides, $P_{\text{AP}} = 20$ dBm, $\sigma^2 = -80$ dBm, $f_c = 2.4$ GHz, the pixel number[7] $M = 200^2$, the realization number is 5000, and Doppler effect is ignored.

[6] We employ $\cos(\cdot)$ as the NF pixel gain function in this paper.

[7] While $M = 200$ is sufficient to demonstrate the benefits of the RIS [12], we choose a larger value for M in this study to ensure a typical NF scenario [3] and to obtain more compelling Monte Carlo results.

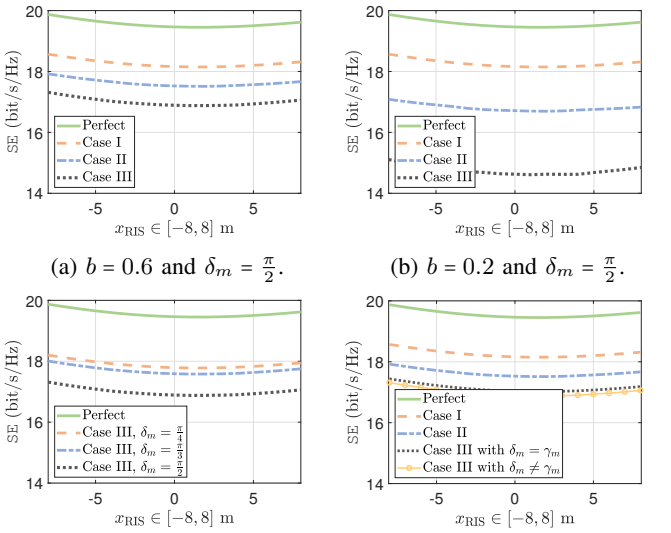

(a) $b = 0.6$ and $\delta_m = \frac{\pi}{2}$. (b) $b = 0.2$ and $\delta_m = \frac{\pi}{2}$.

(c) $b = 0.6$ and $\delta_m = \frac{\pi}{2}$, $\frac{\pi}{3}$, and $\frac{\pi}{4}$. (d) $b = 0.6$. $\delta_m = \frac{\pi}{2}$ and $\gamma_m = \frac{\pi}{2}$ are i.i.d.

Fig. 6: SE for the moving RIS from the AP to the user. Note that $a = 1$, $c = 0.43\pi$, and γ_m is the PE that exists in the PDA.

Fig. 6a shows that Case III performs worst since it considers the PSE and the PDA (with the PE) and their mutual coupling loss. Case II also contains the PSE but the PDA operates without errors. Accordingly, Case I performs better than II and III, this is because it only considers the PSE and $\beta \equiv 1$. The case without the PSE and the PDA, i.e., the first model in Table I, is the error-free baseline. Figure 6b shows that a smaller b in (2) leads to reduced SE. All SEs first decrease and then increase since the RIS performs worst when it is located in the middle between the AP and the user [12]. Fig. 6c shows that the cases with $\delta_m = \frac{\pi}{4}$ and $\frac{\pi}{3}$ perform better than with $\frac{\pi}{2}$, as expected. Lastly, when the PE γ_m in the PDA and δ_m are i.i.d., the performance is the worst, as Fig. 6d illustrates.

V. Conclusion

This paper has studied the mutual coupling effect of the PSE and the PDA with the PE in the RIS-assisted system. The main findings are 1) the PE exists not only in the PSE but also in the PDA, 2) the PE has a more serious impact when the phase shift is far away from the minimal phase and vice versa, and 3) i.i.d. PEs in the PSE and the PDA bring additional uncertainties. Future research prospects include integrating Rician channel modeling the PDA contains the PE, deriving analytical upper bounds on the PL assuming i.i.d. PEs in both the PDA and the PSE, obtaining a closed-form expression of the SE considering the proposed channel model, analyzing the case that the PE follows Von Mises distribution, and comparing the different impacts of the mutual coupling on NF and FF RISs.

Appendix A
Proof of Proposition 2

Because the PDA is a constant β_m, then the second part of (4) can be rewritten as $\left|\text{E}\left\{\beta_m \exp(-\jmath\delta_m)\right\}\right|^2$. Note that β_m is

not a random variable and $\exp(-\jmath\delta_m) = \cos(\delta_m) - \jmath\sin(\delta_m)$, thus we have

$$\begin{aligned}&\left|\mathsf{E}\{\beta_m \exp(-\jmath\delta_m)\}\right|^2 \\ &= \left(\frac{1}{M}\sum_{m=1}^{M}\beta_m\right)^2 \left|\int_{-x}^{x}\cos(\delta_m) f(\delta_m) d\delta_m\right|^2. \end{aligned} \tag{12}$$

Recall that we defined $f(\delta_m) = \frac{1}{2x}$ in Sec. III-A., then $\int_{-x}^{x}\cos(\delta_m)f(\delta_m)d\delta_m = \frac{1}{2x}\int_{-x}^{x}\cos(\delta_m)d\delta_m = \frac{\sin(x)}{x}$. Therefore, $\left|\mathsf{E}\{\beta_m \exp(-\jmath\delta_m)\}\right|^2 = \left(\frac{1}{M}\sum_{m=1}^{M}\beta_m\right)^2\left(\frac{\sin(x)}{x}\right)^2$. Lastly, by using Taylor series expansion $\sin(x) = x - \frac{1}{6}x^3 + \frac{1}{120}x^5 + o(x^7)$ [18], (5) is obtained. Consequently, we have

$$\begin{aligned}&\frac{\partial}{\partial x}\left\{\left|\mathsf{E}\{\beta_m \exp(-\jmath\delta_m)\}\right|^2\right\} \\ &\approx \left(\frac{1}{M}\sum_{m=1}^{M}\beta_m\right)^2\left(-\frac{2}{3}x + \frac{8}{45}x^3 - \frac{1}{60}x^5 + \frac{1}{1800}x7\right). \end{aligned} \tag{13}$$

Let (13) < 0, we have $x \in (0, 3.162)\bigcup(-\infty, -3.162)$. Note that $x \in \left(0, \frac{\pi}{2}\right) \subset (0, 3.162)$, then we can see that the phase error δ_m decreases (5). In other words, when x increases, (5) decreases.

Appendix B
Proof of Proposition 3

Based on the equivalent phase shift model in Sec. II., we can find that (2) reaches the upper bound when $a = 1$. Therefore, we have $\left|\mathsf{E}\{\beta(\phi_m)\exp(-\jmath\delta_m)\}\right|^2 \le \left|\mathsf{E}\{\bar{\beta}(\phi_m)\exp(-\jmath\delta_m)\}\right|^2$. Then $\zeta = \left(\frac{(1-b)}{2}\sin(\phi_{mn} - c) + \frac{(1+b)}{2}\right)^2$ and $\frac{\partial}{\partial x}\left\{\left|\mathsf{E}\{\bar{\beta}(\phi_m)\cdot\exp(-\jmath\delta_m)\}\right|^2\right\} \approx \zeta(-\frac{2}{3}x + \frac{8}{45}x^3 - \frac{1}{60}x^5 + \frac{1}{1800}x^7)$. The rest proof is similar to Appendix A.

Appendix C
Proof of Proposition 4

From Appendix B, it can be seen that we only need to study the case with $a = 1$, thus $\left|\mathsf{E}\{\bar{\beta}(\phi_m + \delta_m)\exp(-\jmath\delta_m)\}\right|^2 = \left|\frac{1}{2x}\int_{-x}^{x}\bar{\beta}(\phi_m + \delta_m)\cos(\delta_m)d\delta_m - \frac{\jmath}{2x}\int_{-x}^{x}\beta(\phi_m + \delta_m)\sin(\delta_m)d\delta_m\right|^2$. Note that $\int_{-x}^{x}\beta(\phi_m + \delta_m)\cos(\delta_m)d\delta_m = \frac{(1-b)}{2}\sin(\phi_m - c)\left(x + \frac{1}{2}\sin(2x)\right) + (1+b)\sin(x)$, and $\int_{-x}^{x}\beta(\phi_m + \delta_m)\sin(\delta_m)d\delta_m = \frac{(1-b)}{4}(2x - \sin(2x))\cos(\phi_m - c)$. Hence (7) can be obtained easily. Consequently, without loss of generality, we assume $\sin(\phi_m - c) = 0$, then $\left|\mathsf{E}\{\bar{\beta}(\phi_m + \delta_m)\exp(-\jmath\delta_m)\}\right|^2 \approx \frac{(1+b)^2}{4}\left(1 - \frac{1}{6}x^2 + \frac{1}{120}x^4\right)^2 + \frac{(1-b)^2}{4}\left(\frac{1}{3}x^2 - \frac{1}{15}x^4\right)^2$. Hence we have

$$\begin{aligned}&\frac{\partial}{\partial x}\left\{\left|\mathsf{E}\{\bar{\beta}(\phi_m + \delta_m)\cdot\exp(-\jmath\delta_m)\}\right|^2\right\} \\ &= -\frac{(1+b)^2}{6}x + \varrho_1 x^3 - \varrho_2 x^5 + \varrho_3 x^7, \end{aligned} \tag{14}$$

where $\varrho_1 = \frac{2(1+b)^2+5(1-b)^2}{45}$, $\varrho_2 = \frac{(1+b)^2+16(1-b)^2}{240}$, and $\varrho_3 = \frac{(1+b)^2+64(1-b)^2}{7200}$. Let (14) equals 0, and recall $b \in [0,1]$, then for $x \in \left[0, \frac{\pi}{2}\right]$, there is only one real solution $x = 0$. Because of the continuity [18], for $b \in [0,1]$, the only real solution is also $x = 0$. Other real roots are $x_2 = -2.286$ and $x_3 = 2.286$ if $b = 0$. It is not difficult to verify that when $x \in (0, x_3 = 2.286)\bigcup(-\infty, x_2 = -2.286)$, (14) < 0, and $(0, x_3 = 2.286) \supset \left(0, \frac{\pi}{2}\right)$. Similarly, the cases that $b \in (0,1]$ and $\sin(\phi_m - c) < 0$ ($\sin(\phi_m - c) > 0$) can be analyzed as the case above. The proof is completed.

References

[1] G.-B. Wu, J. Y. Dai, K. M. Shum, K. F. Chan, Q. Cheng, T. J. Cui, and C. H. Chan, "A universal metasurface antenna to manipulate all fundamental characteristics of electromagnetic waves," *Nature Communications*, vol. 14, no. 1, p. 5155, 2023.

[2] V. G. Ataloglou, S. Taravati, and G. V. Eleftheriades, "Metasurfaces: Physics and applications in wireless communications," *National Science Review*, vol. 10, no. 8, 2023.

[3] Y. Liu, Z. Wang, J. Xu, C. Ouyang, X. Mu, and R. Schober, "Near-field communications: A tutorial review," *IEEE Open J. Commun. Soc.*, vol. 4, pp. 1999–2049, 2023.

[4] P. Ramezani and E. Björnson, "Near-field beamforming and multiplexing using extremely large aperture arrays," in *Fundamentals of 6G Communications and Networking*. Springer, 2023, pp. 317–349.

[5] M.-A. Badiu and J. P. Coon, "Communication through a large reflecting surface with phase errors," *IEEE Wireless Commun. Lett.*, vol. 9, no. 2, pp. 184–188, 2020.

[6] S. Zhou, W. Xu, K. Wang, M. Di Renzo, and M.-S. Alouini, "Spectral and energy efficiency of IRS-assisted MISO communication with hardware impairments," *IEEE Wireless Commun. Lett.*, vol. 9, no. 9, pp. 1366–1369, 2020.

[7] D. Yang, J. Xu, W. Xu, B. Sheng, X. You, C. Yuen, and M. Di Renzo, "Spatially correlated RIS-aided secure massive MIMO under CSI and hardware imperfections," *IEEE Trans. Wireless Commun., to appear*, 2024.

[8] S. Abeywickrama, R. Zhang, Q. Wu, and C. Yuen, "Intelligent reflecting surface: Practical phase shift model and beamforming optimization," *IEEE Trans. Commun.*, vol. 68, no. 9, pp. 5849–5863, 2020.

[9] M. A. Mosleh, F. Héliot, and R. Tafazolli, "Ergodic capacity analysis of reconfigurable intelligent surface assisted MIMO systems with a practical phase shift and amplitude response," *IEEE Trans. Veh. Technol., to appear*, 2024.

[10] C. Ozturk, M. F. Keskin, H. Wymeersch, and S. Gezici, "RIS-aided near-field localization under phase-dependent amplitude variations," *IEEE Trans. Wireless Commun.*, vol. 22, no. 8, pp. 5550–5566, 2023.

[11] K. Wang, C.-T. Lam, and B. K. Ng, "How long can RIS work effectively: An electronic reliability perspective," in *2023 IEEE 98th Vehicular Technology Conference (VTC2023-Fall)*, 2023, pp. 1–6.

[12] E. Björnson, O. Özdogan, and E. G. Larsson, "Intelligent reflecting surface versus decode-and-forward: How large surfaces are needed to beat relaying?" *IEEE Wireless Commun. Lett.*, vol. 9, no. 2, pp. 244–248, 2020.

[13] O. Özdogan, E. Björnson, and E. G. Larsson, "Intelligent reflecting surfaces: Physics, propagation, and pathloss modeling," *IEEE Wireless Commun. Lett.*, vol. 9, no. 5, pp. 581–585, 2020.

[14] H. Taghvaee, S. Abadal, J. Georgiou, A. Cabellos-Aparicio, and E. Alarcón, "Fault tolerance in programmable metasurfaces: The beam steering case," in *2019 IEEE International Symposium on Circuits and Systems (ISCAS)*, 2019, pp. 1–5.

[15] H. Taghvaee, A. Cabellos-Aparicio, J. Georgiou, and S. Abadal, "Error analysis of programmable metasurfaces for beam steering," *IEEE J. Emerg. Sel. Top. Circuits Syst.*, vol. 10, no. 1, pp. 62–74, 2020.

[16] X. Pei, H. Yin, L. Tan, L. Cao, Z. Li, K. Wang, K. Zhang, and E. Björnson, "RIS-aided wireless communications: Prototyping, adaptive beamforming, and indoor/outdoor field trials," *IEEE Trans. Commun.*, vol. 69, no. 12, pp. 8627–8640, 2021.

[17] H. Friis, "A note on a simple transmission formula," *Proceedings of the IRE*, vol. 34, no. 5, pp. 254–256, 1946.

[18] I. S. Gradshteyn and I. M. Ryzhik, *Table of integrals, series, and products*. Academic press, 2014.